

Chapter 5. Compression and Indentation Damage Mechanics of FA Reinforced PU Foam Core

This chapter presents a comprehensive study on neat and FA-PUF under compression is included in this work. The effect of reinforcement on the deformation behavior of the PUF with varying wt. percentage of the FA is discussed in detail. An elaborated investigation of the indentation damage behavior of the fabricated polymeric foam with specific FA reinforcement has been carried out. Damage analysis due to the quasi-static loading of indenters with flat-circular, hemispherical, and conical nose shapes on neat PUF and FA reinforced PUF with varying weight percentages has been discussed. Multiple factors that influence indentation resistance have been identified and reported. The results are then corroborated with the SEM images of the cross-sectional cut of the damaged foam under indentation with various nose shapes. The variation in indentation resistance offered by the reinforced PUF for different nose tip profiles of the indenter has been explained with graphical observations.

5.1. Mechanical Characterization

The evaluation and scientific interpretation of the observations are carried out consistent with existing literature on the damage behavior of other material configurations. In this section compressive stress characteristics are elaborated for different specimens. This study highlights the quasi-static indentation of core material, including a neat PUF core and fly ash loaded PUF core.

5.1.1. Compression Testing of PUF Core

The compression testing is performed on the fabricated PUF foam core coupons to evaluate their capability to sustain load under compression. The testing parameters and specimen dimensions are set according to the ASTM C365/C365M. The result of compression testing

is the average value of three test specimens of the same composition under the same testing parameters. The inclusion of fly ash varying by weight to the PUF core is 5%, 10%, 15% and 20%, respectively. Thereafter, the compression test is conducted on the specimen of each composition.

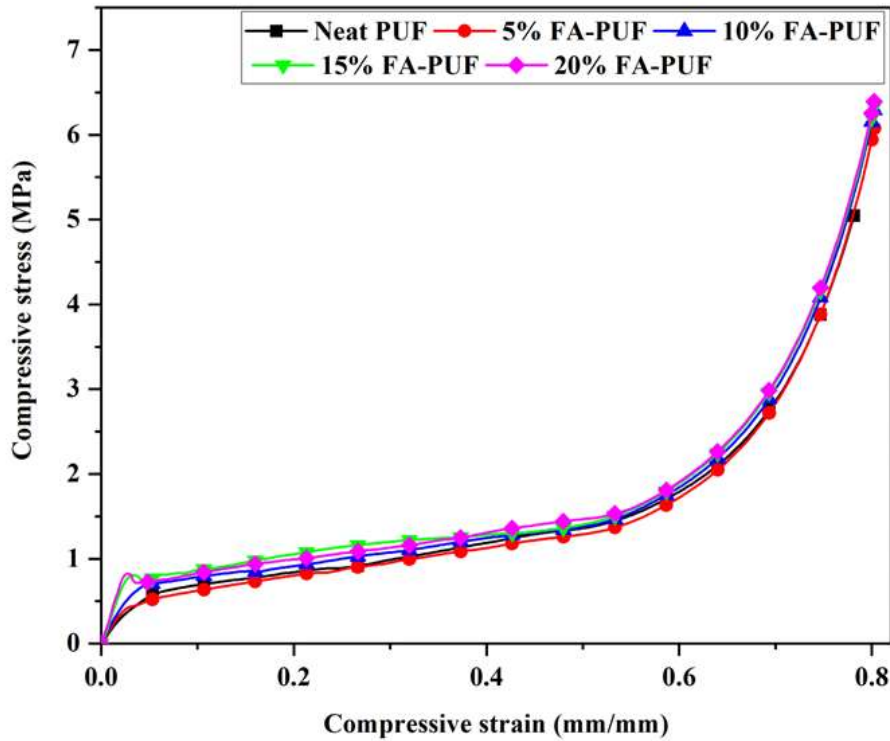


Figure 5.1 Stress-strain curve of neat and reinforced FA-PUF under compression.

The curve shown in figure 5.1 is the classic compressive stress-strain curve representing closed-cell foam's elastomeric nature. The curve acts linear elastic in the beginning, followed by a long plateau that further changes to a sharp rise at the end. The curve goes through three phases, and these three phases are associated with the deformation behavior of the cellular structure of the closed-cell foam. In this case, the curve is linear at lower stresses. The deformation is linear elastic, primarily because cell edges bend and walls stretch simultaneously. If the applied load is removed, it regains its original position. The second phase is the most prolonged here. The cell starts to buckle elastically and mostly collapses

plastically; therefore, it is called a collapse plateau. When the cells are continuously collapsing and about to touch the opposite wall of the cells, stress value increases rapidly with respect to strain. This rise in stress value shows the densification of the solid. This densification represents the third phase of the compression curve [207].

The stress-strain behavior can be better explained with the enlarged part of the compression curve as shown in figure 5.2, delineating the elastic and part plastic regions up to 0.1 (mm/mm) strain. The slope of the linear part of each curve represents the modulus of elasticity. The curve shows that there is an increment in yield strength and elastic modulus with fly ash inclusion with the exception that the yield strength of the 5% FA-PUF is less than the neat PUF.

Since the PUF fabrication mold has a constant volume cavity, as the fly ash inclusion increases with respect to the polyurethane by weight, the cell density also increases. This affects the thickness of the cell walls and cell struts. Therefore, the stress carrying capacity of the solid foam decreases due to the reduction in the dimension of cell walls and struts. Hence the compressive yield property of the 5% FA-PUF degrades. This degradation phenomenon has also been established elsewhere in the previously published work [208]. Further, the compressive properties increase with the fly ash inclusion in the PUF. The average elastic modulus as obtained experimentally is listed in Table 5.1.

Table 5.1 Neat and FA- PUF's properties under compression.

Foam type	Young's modulus (MPa)	Yield stress (MPa)	Yield strain
Neat PUF	16.78	0.59	0.0586
5% FA-PUF	19.44	0.43	0.032
10% FA-PUF	23.20	0.69	0.0426
15% FA-PUF	34.58	0.80	0.032
20% FA-PUF	37.28	0.81	0.0305

The linear part shows the elastic deformation of the PUF and FA-PUF, which progresses to the plateau region. The transformation from linear elastic to plateau region is smooth for neat PUF, 5% FA-PUF and 10% FA-PUF. The same is not with 15% FA-PUF and 20% FA-PUF. The shift from linear elastic region to plateau goes through a sudden drop in stress value which shows the swift collapse of the cells. The increase in stiffness gives rise to the abrupt collapse of the cellular structure. As a result, heavily reinforced PUF has a distinct nature than poorer reinforced PUF.

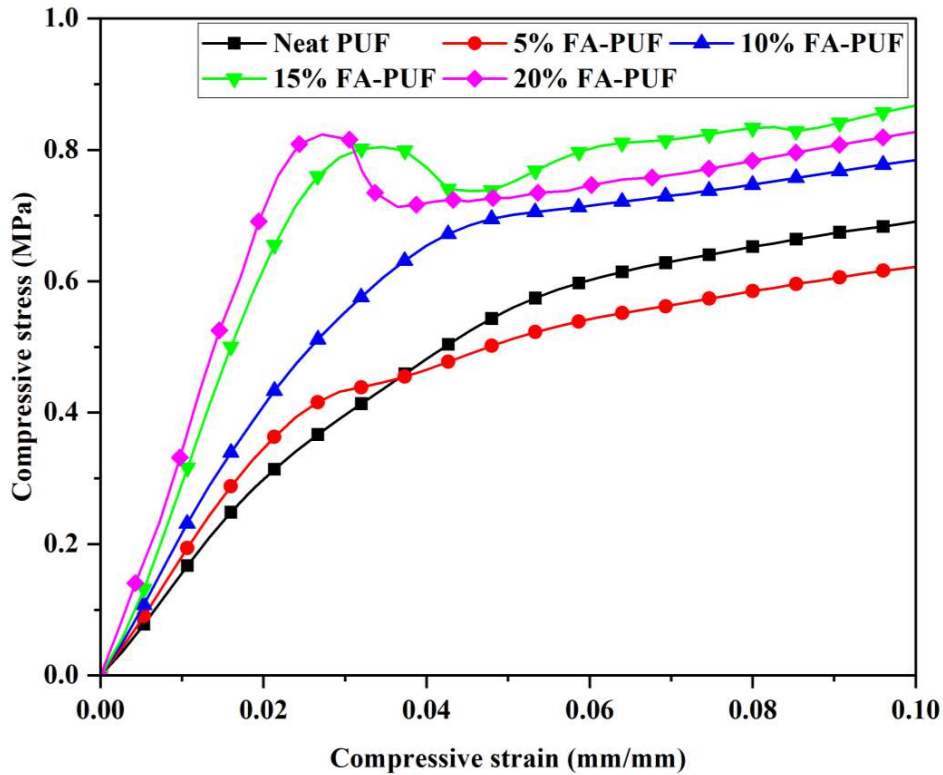


Figure 5.2 Elastic to plastic behavior of neat and reinforced FA-PUF core under compression.

5.1.2. Quasi-Static Indentation Test

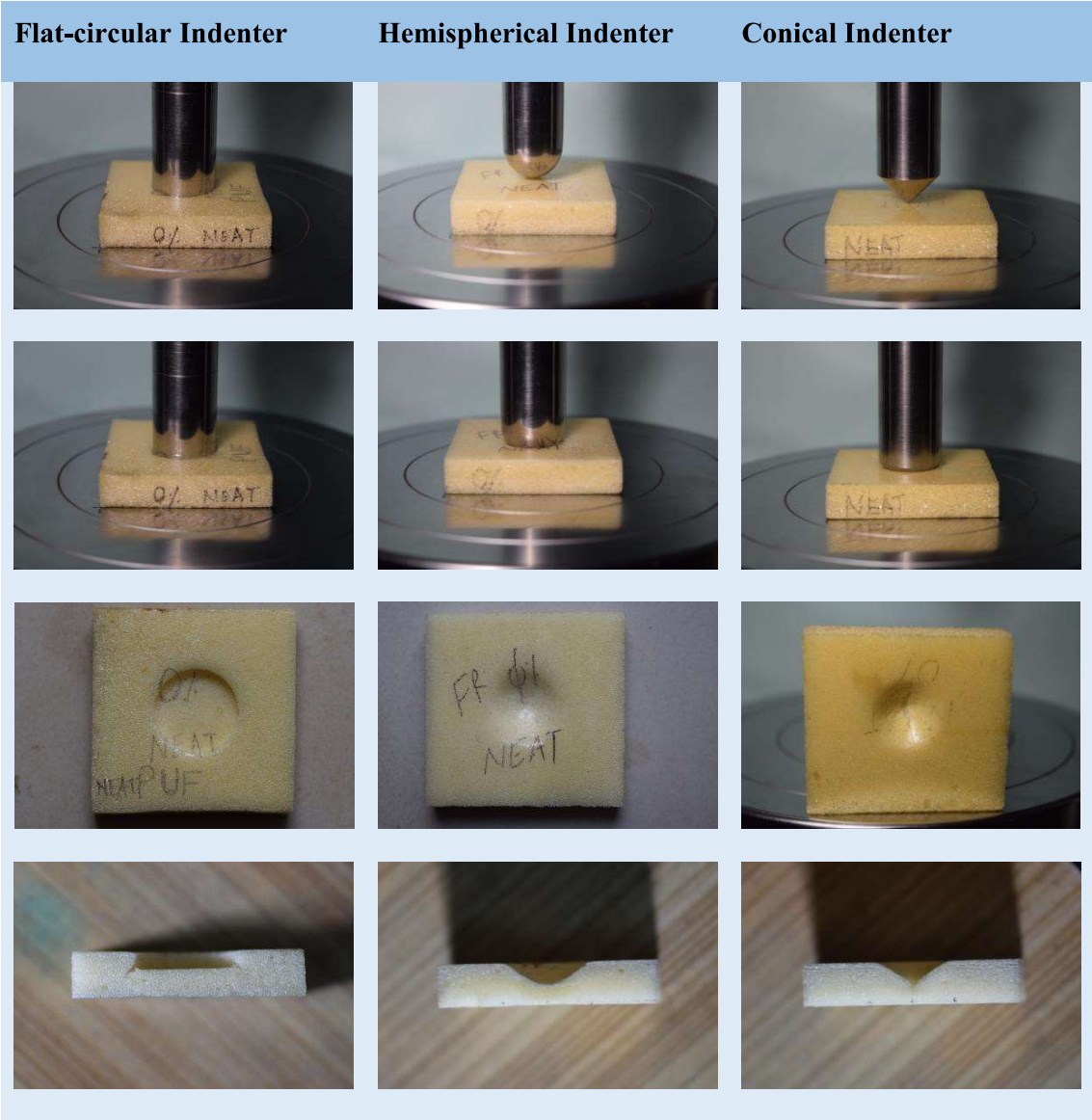


Figure 5.3 Experimental setup and deformation incurred on Neat PUF by the flat-circular, hemispherical and conical indenter.

In sandwich composites, the face sheet is clubbed to a low-density core material for enhancing its out-of-plane load carrying capabilities. Because the face sheet alone is susceptible to out-of-plane loading, strategically, it becomes essential to understand the behavior of the core material first. The quasi-static indentation test has been performed on the neat PUF core and FA-PUF core. This test is conducted to study the indentation

resistance of the neat and FA reinforced foam core. As shown in figure 5.3, the effect of geometry on indentation resistance is evaluated using three different types of indenter nose shapes. The cut cross-sections of the indented neat PUF are also shown for better apprehensibility of the damage incurred.

It's critical to comprehend how the indentation develops in the foam core and leads to a dent. The resisting force is seen to increase with the indentation depth during experimentation. However, the pattern of the force variation with indentation is mainly reliant on the geometry of the indenter tip. The load vs indentation curve characteristics is dependent not just on the nose geometry but also controlled by the deformation behavior of the reinforced PUF core. Therefore, it is necessary to study the effect of reinforcement on the deformation behavior under different nose shape indentation, which also contributes to the indentation resistance behavior.

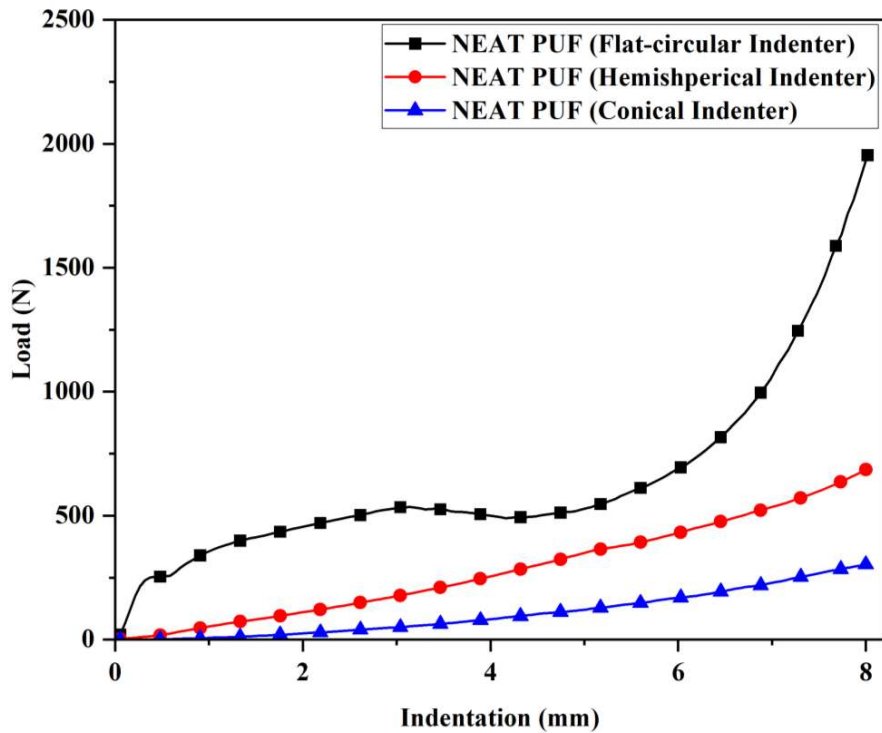


Figure 5.4 Load-Indentation curve behavior of Neat PUF core under flat-circular, hemispherical and conical indenter tip shape.

The indentation response on neat PUF by different indenters is plotted in figure 5.4. The nature of variation corresponding to each indenter is unique. The distribution shows the effect of nose shape on force interaction to indentation depth. The load variation with respect to the depth of indentation is influenced by the deformation behavior of the closed-cell PUF. From the Load-Indentation curve, it is clear that initially, elastic deformation at lower strains occurs until it reaches the crest and then the onset of plastic collapse and crushing of cells begins. The rise in the load value in the plastic region suggests more work is needed to tear the cell wall at the contact site of the PUF and flat-circular indenter. Then after, there is a drop in load value with indentation. After the cell wall ruptures along the circular edges, the cylindrical surface area of the indenter is exposed to the foam, causing friction opposite to the indentation direction. This might also have contributed to the rise in indentation resistance. Further, the load increases rapidly, indicating the densification of the closed-cell PUF backed by rigid support. The indentation resistance offered by the foam to the hemispherical indenter lies in between the flat-circular and conical indenter. Initially, it shows an elastic increment with load, but the gradient of the curve is lower than the flat-circular indenter but higher than the conical indenter. For the same target PUF material, the indentation response shows that the value of resistive force also changes with the nose geometry.

At different indentation points, three resistive forces: tearing force, crushing force, and shear force or friction force, come into play. First, the tearing force is exerted at the point of contact. But the hemispherical geometry is a smooth curved surface that acts as a blunt indenter. The foam core surface deforms and takes the shape of an indenter tip and experiences crushing force. The curve shows the initial elastic regime. Further indentation travel includes the tearing force also. The linear behavior shows the elastic deformation of

the PUF core followed by the plastic crushing of the core. The curve slope shows a slight dip due to the plastic crushing of the PUF core. The curve continues to progress with increasing slope, pushing foam under plastic crushing and working to tear the cell wall. However, there is a depression in the load value near 5 mm indentation depth. Here, the tearing of the foam core degrades the resistive characteristics of the PUF core. Densification of the core occurs as the indentation progresses and pushes the foam core against the rigid support. Densification of the foam core causes the indentation load to shoot up rapidly.

Contrastingly, for the case with a conical indenter, the curve shows that the indentation resistance value is the least for the conical indenter. The low value of indentation load is because of the sharp tip of the conical indenter. It tears the cell wall at the point of contact and travels through the foam core. Little resistance under the indenter tip initially makes it easy to puncture through the foam core and supports the low load value in the early stage of the load-indentation curve. It shows conical tip predominantly confronted tearing resistance offered by the PUF core. However, as the indenter progresses into the foam core, more surface area gets in contact with the foam, boosting indentation resistance. Apart from the tearing resistance, crushing and shear resistance are also significant determinants in indentation nose geometry study. Crushing resistance is provided by the region surrounding the tip of the indenter. It increases with indentation depth, whereas shear resistance is induced by friction at the conical indenter-foam core interface. Consequently, the area of contact with the foam core increases corresponding to the indentation depth, increasing indentation resistance. As a result, the Load-Indentation curve has a parabolic shape. The curve does not capture the densification phenomena because the densification zone is relatively small, just under the indenter tip. Therefore, its contribution to the nature of the curve is trivial.

Figure 5.5 summarises the elaborated discussion of how the deformation mechanism and deformation zones vary with the indentation geometry. For flat-circular indenter, resistance due to crushing is prominent (Figure 5.5 (a)), whereas for hemispherical indenter, elastic buckling and plastic crushing are prominent factors to resist the indentation (Figure 5.5 (b)). As shown in Figure 5.5 (c) for conical indenter, the deformation is dominated by tearing of foam core and resistance offered is minimal.

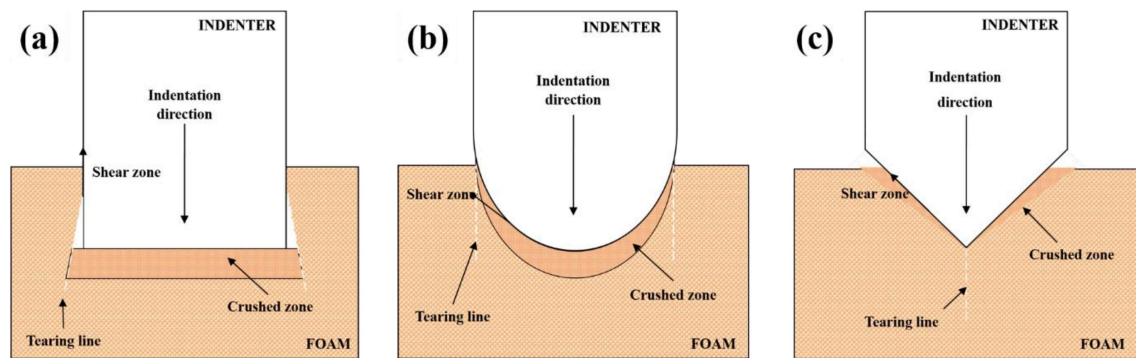


Figure 5.5 Deformation characteristics of the foam core for (a) flat-circular (b) hemispherical, and (c) conical indenter.

This study is focused on the effect of nose shape on foam core indentation behavior and critically the influence of nose shape on PUF core reinforcement. Research works on the later part are a few in the public domain. This study examines the impact of reinforcement on indentation resistance provided by indenters with different nose tip shapes. The effect of reinforcement with respect to each indenter nose tip shape has been evaluated for different combinations. The sequence of the study is as follows at first, the flat-circular indenter is considered to study its effect on neat and reinforced FA-PUF. Then hemispherical indenter nose tip is used, followed by the conical tip indenter. From a single fabricated FA-PUF sheet, three ASTM specimens are prepared respective to three indenters and the same is repeated for 5%, 10%, 15% and 20% fly ash inclusion sheets.

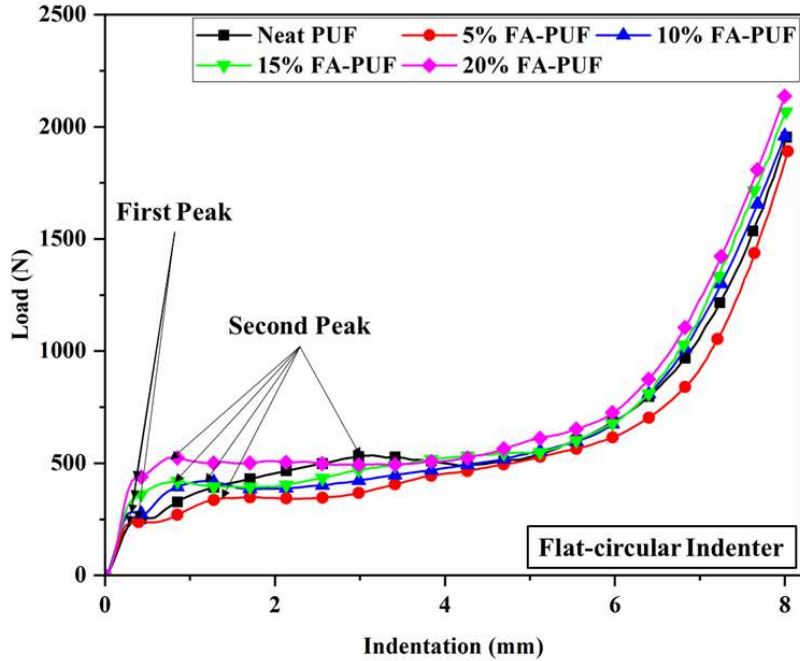


Figure 5.6 Load-Indentation curve of neat and reinforced FA-PUF core under the flat-circular indenter.

The Load-Indentation curve for a neat and reinforced PUF core under a flat-circular indenter is shown in figure 5.6. The curve depicted is a variant of the compression test curve discussed in section 4.2. The neat and reinforced foam initially exhibits elastic behavior, followed by a prolonged plateau indicating plastic crushing of the closed cells. Finally, a surge in the load value is observed due to the densification of the foam core. The indentation sequence through the PUF core is similar to the compression curve. However, closer inspection reveals two peaks in the plateau region, unlike the compression curve. The first peak indicates the beginning of plastic core crushing. As the flat-circular indenter progresses further, more work is required to tear the cell wall along the periphery of the flat-circular indenter. Hence, this rise in the load leads to the second peak. Then, the indenter tears the PUF core along the line of contact. There is a loss in load value due to cell wall tearing and the indenter punctures the PUF core. The rest of the deformation mechanism is well aligned with the compression deformation mechanism. Another point to notice from the graph is that when PUF is reinforced with FA particles, the time between the first and second peaks gets shorter.

With the incremental wt.% addition of FA to PUF, the PUF foam becomes less flexible and hence the above behavior might have been observed.

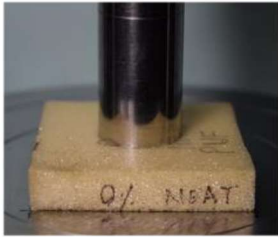
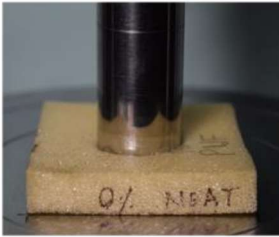
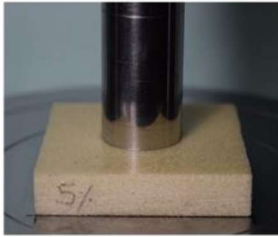
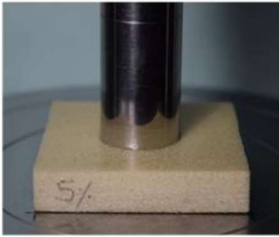
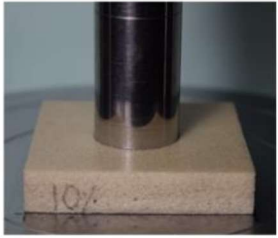
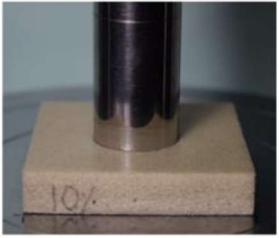

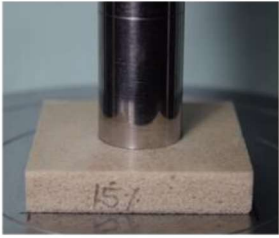
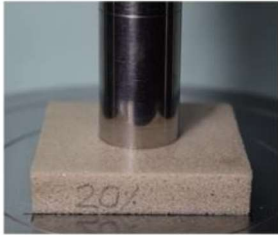
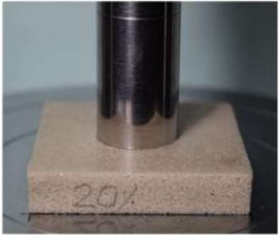
First Peak Load	Second Peak Load
 <p>Load: 250.16 N Indentation: 0.37 mm</p>	 <p>Load: 534.81 N Indentation: 3.13 mm</p>
 <p>Load: 234.38 N Indentation: 0.28 mm</p>	 <p>Load: 344.32 N Indentation: 1.38 mm</p>
 <p>Load: 282.15 N Indentation: 0.31 mm</p>	 <p>Load: 420.26 N Indentation: 1.17 mm</p>
 <p>Load: 336.01 N Indentation: 0.32 mm</p>	 <p>Load: 419.56 N Indentation: 0.85 mm</p>
 <p>Load: 437.83 N Indentation: 0.37 mm</p>	 <p>Load: 525.41 N Indentation: 0.8 mm</p>

Figure 5.7 The first and second peak load and corresponding indentation depth for flat-circular indenter to varying wt. % FA-PUF.

Table 5.2 Peak values of the neat and FA-PUF core under flat-circular indentation.

Foam type	First peak load (N)	Indentation depth (mm)	Second peak load (N)	Indentation depth (mm)
Neat PUF	250.16	0.37	534.81	3.13
5% FA-PUF	234.38	0.28	344.32	1.38
10% FA-PUF	282.15	0.31	420.26	1.17
15% FA-PUF	336.01	0.32	419.56	0.85
20% FA-PUF	437.83	0.37	525.41	0.8

The first peak appears at the end of the elastic limit, while the second appears just before the onset of cell wall tearing. These two peaks are represented in figure 5.7 with a real-time experimental picture and its orthographic schematic projection maintaining the accurate aspect ratio. This figure represents the influence of FA reinforcement on the load-bearing capacity of PUF and the respective indentation depth. The whole data is summarised in table 5.2. The value of the load and indentation depth clearly shows the influence of reinforcement on PUF. In case of first peak load corresponding, indentation depth increases with FA inclusion to PUF. On the contrary, indentation depth corresponding to the second peak load decreases with FA wt. % to PUF.

With reference to figure 5.8, the sequence of the interaction of the hemispherical indenter to the PUF foam core can be divided into three parts. The first part of the curve starts with elastic deformation and the slope proceeds to the plastic crushing of the foam core. The second part of the curve, where the slope recedes, shows the interaction of the indenter's hemispherical profile to the PUF core, and the third part is the densification of the core. In the second part, immersion of the indenter into the foam core increases the foam core's contact area with the indenter. The immersion and increase in the contact area of the indenter govern the deformation mechanism of the PUF core.

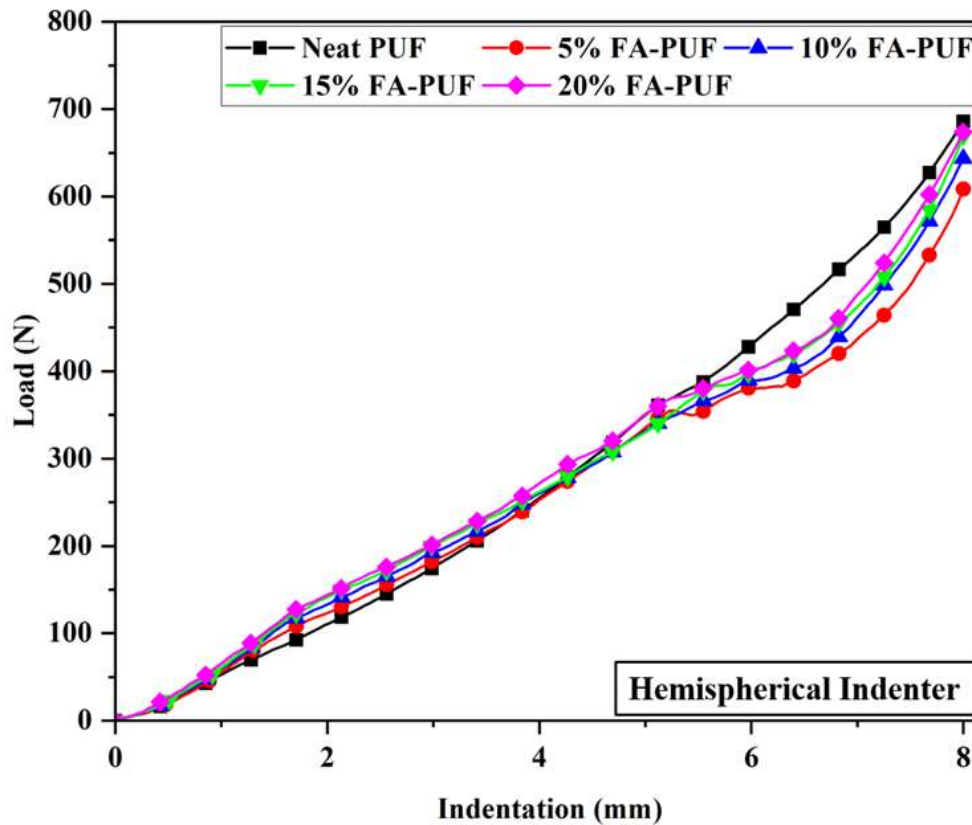


Figure 5.8 Load-Indentation curve of neat and reinforced FA-PUF core under the hemispherical indenter.

After an initial constant slope, the recession in slope of the curve in the second part depicts the plastic crushing of the cellular structure. However, the progressive new contact areas generated due to further penetration are governed by elastic deformation. Therefore, the plateau, which is evident in the case of compression and indentation under a flat-circular indenter, is not the same for the hemispherical indenter. The plastic crushing of the core was accompanied by the elastic deformation of the core, which has resulted in a linear profile of the curve but with a lesser slope. After indenting foam to 5 mm depth, a drop in load indicates the foam core's tearing under the indenter projected area. The drop in the load is more significant in the reinforced PUF than the neat PUF indicating the increment in the rigidity

of the PUF core with reinforcement. At the end of the second phase, tearing of the foam core initiates and consequently, the third phase of the curve shows the surge in load value depicting the densification of the core against a rigid support.

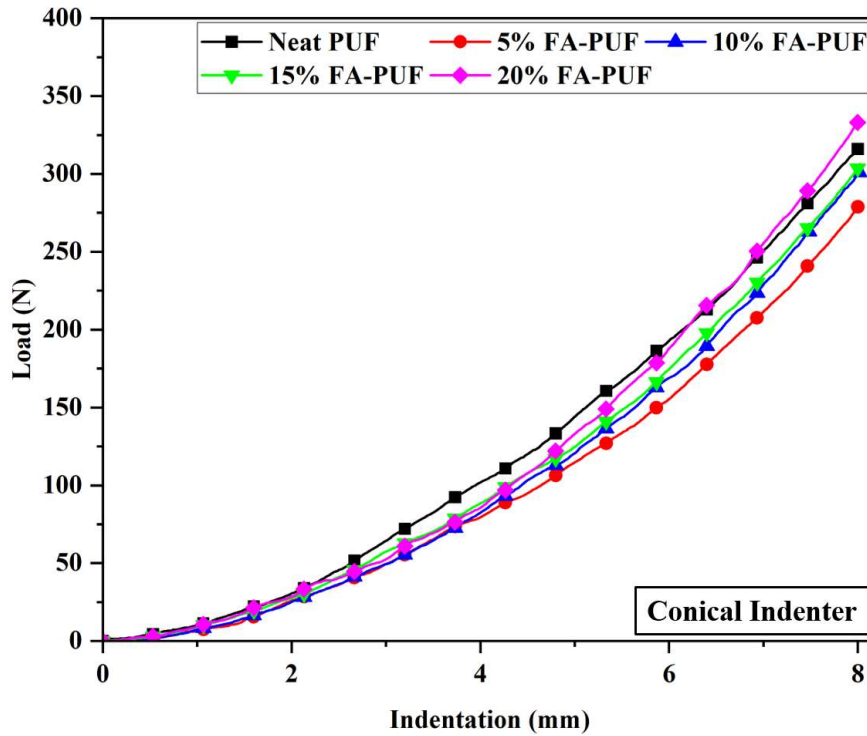


Figure 5.9 Load-Indentation curve of neat and reinforced FA-PUF core under the conical indenter.

The attributes of the conical indenter curve are significantly different from those of the other two curves, as shown in figure 5.9. Resistance to indentation offered by the PUF core is much less as reflected by the load values on ordinate with respect to the depth of penetration on the abscissa. It is pertinent to rethink the deformation sequence of the PUF core under a conical indenter. As the indenter begins to tear the core with its sharp nose tip, it starts ripping the foam core from the beginning. But as the indenter travels through the foam core, the resistance to indentation increases rapidly. This is because more surface area comes into contact with foam core because of the profile of the conical nose tip. The increment in resistance is due to the shear or friction force increment at the core and conical profile

interface. In addition to the shear force, core crushing also contributes to the indentation resistance capability as evident from the huge curve slope upsurge. So, the deformation sequence in the case of conical indenter starts with a tearing of the core followed by the crushing and shearing of the foam core. From the load-indentation curve, it is evident that the neat PUF outperforms the reinforced PUF. This is because the neat foam core is more flexible, blends the conical profile shape more efficiently and offers more resistance against the indentation than the stiffer FA reinforced PUF core. But as indentation proceeds through the core, crushing and shearing resistance contributes more against the penetration. Hence the indentation resistance as reflected by the gradients of the Load - Indentation curve, is higher for the reinforced PUF than the neat PUF.

5.2. Cross-section Examination of Damaged PUF Core

The test coupons are cut perpendicular to the plane of the PUF core along the center of the indentation cavity with the help of a diamond cutter after the completion of testing neat and FA reinforced PUF core against indentation with three different indenters. The micro images were taken to study the damage mechanics of the neat PUF and FA-PUF under different nose tip profiles of the indenter. The nature of the curve can be justified by the cross-section images of the neat PUF and FA reinforced PUF. It was impossible to take micro images of full-length damaged cross-sections in one go. Therefore, pictures were taken in part due to the magnification limitation of the stereoscopic microscope. The images were taken with a 10x zoom lens in three parts of the total damage portion from right to left. The specimen was marked so that putting these pictures back together would be simple. The damaged cross-sections of the neat PUF and FA-PUF under the flat-circular indenter are shown in figure 5.10. The figure shows that the foam core's bounce-back capability was reduced with the fly ash inclusion. Therefore, the residual thickness under the flat-circular indenter for the neat PUF is more than the reinforced PUF. The deformed area represented by the blue outline in

the images is seen to change with the amount of reinforcement inclusion. The affected area under the flat-circular indenter for the neat PUF is more and recedes with the reinforcement in the PUF core. The tearing line indicates the characteristic of foam core, varying from more flexible to brittle from Neat PUF to FA-PUF. The tearing line converges with FA reinforcement to the PUF under the flat-circular indenter. Tearing line convergence reduces the time between the load drop after elastic crushing and tearing of PUF core in the Load-Indentation curve under the flat-circular indenter.

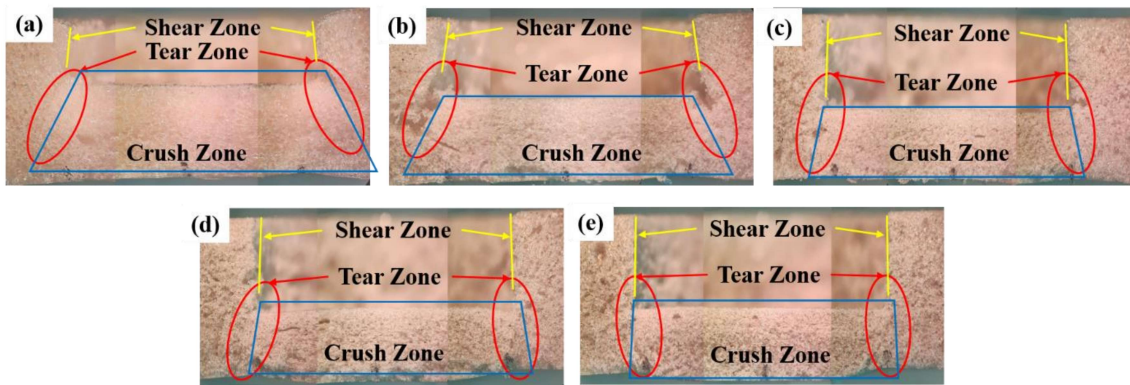


Figure 5.10 Cross-section of indented (a) neat PUF, (b) 5%, (c) 10%, (d) 15% and (e) 20% FA-PUF under flat-circular indenter.

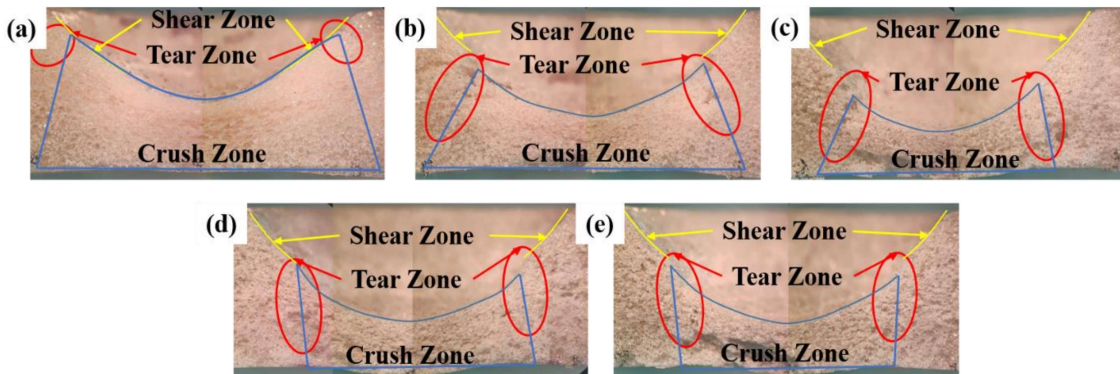


Figure 5.11 Cross-section of indented (a) neat PUF, (b) 5%, (c) 10%, (d) 15% and (e) 20% FA-PUF under hemispherical indenter.

The PUF foam core deforms utmost under the hemispherical profile indenter, especially at the tip zone, as shown in figure 5.11. The core crushing is seen to start near the tip and subsequently extends away from the center along the hemispherical profile of the indenter.

The tearing starts when the indenter travels up to a certain depth. In this case, the tearing starts after 5mm of indentation depth. Due to tearing, the indentation resistance drops yet is sustained by the core crushing and shear resistance offered by the PUF core. The crushing of the core is not only confined within the tear line (crushing zone), but it also spreads beyond the shear zone where the surface area of the indenter keeps pushing the core. The resistance is due to the shear force acting between the PUF core and the indenter interface.

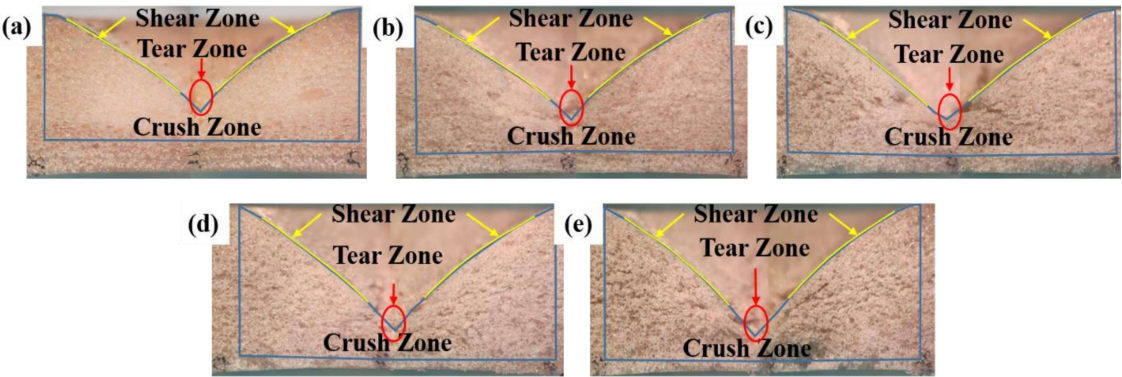


Figure 5.12 Cross-section of indented (a) neat PUF, (b) 5%, (c) 10%, (d) 15% and (e) 20% FA-PUF under conical indenter.

Figure 5.12 illustrates the deformation mechanism for the neat PUF and FA-PUF core due to the indentation of the conical profile indenter. Initially, it punctures the surface of the core by tearing and crushing simultaneously with its sharp tip. Because the surface in contact with the indenter is initially minimal, the resistance generated by the PUF core is also quite limited. Since the neat PUF core is more flexible than the reinforced PUF, the deformation spread is more uniformly distributed than FA-PUF core. The tearing resistance against indentation for the neat PUF is higher than that of the reinforced PUF. This is also evident from the initial part of the Load-Indentation curve (Figure 5.9), where the tearing mechanism is more dominant than crushing and shearing. However, as the indenter proceeds through the PUF core, the degree of surface area in contact multiplies. In addition, the higher volume affected by crushing and the larger surface area induced by shear provide more resistance to

the indentation. Therefore, towards the later stages with the increase in fly ash reinforcement inclusion, the indentation resistance of the FA-PUF core supersedes that of the neat PUF core.

The afore-mentioned discussions of the indented cross-sectional images summarise that though the indenter geometry largely influences the indentation resistance offered by the foam core composites, but the pattern of damage progression and mixed-mode nature of tearing, shearing and crushing are significantly different from indenter to indenter and neat PUF to FA-PUF. Also, the dominant deformation mechanism comes at various stages of indentation depth, signifying the criticality of the indenter profile and fly ash inclusion. It is concluded that the flat indenter largely crushes the foam core, while this is not the case with the hemispherical indenter. Here crushing is accompanied by the shear and tearing of the foam core. But as the indenter geometry changes to conical, the tearing of the foam is prominent during the travel through the foam core.

5.3. SEM Micrograph Study

The interpretations from the study are also correlated with the SEM images shown in figure 5.13, 5.14, and 5.15 for the flat-circular, hemispherical, and conical indenter respectively. The foam core chosen for this study is 20% weight fly ash (FA) inclusion composition with neat PUF (20% FA-PUF). The fly ash (FA) particulates are used in this study to reinforce the polyurethane foam (PUF) core.

The foam core primarily offers the damage resistance due to the core crushing, followed by the tearing for a flat-circular indenter. Figure 5.13 shows the half part of the cross-sectional cut of the deformed PUF core under the flat-circular indentation. The magnified figure on the left illustrates that the cell walls and struts are torn down and separated. The tear line propagation divides the projected area under the indenter and the rest of the core material. The compression is experienced only by the cells under the projected area confined by the

tearing line. The enlarged view on the right of figure 5.13 demonstrates severe crushing of the cellular structure, which confirms the densification of the PUF core. The cellular structure of the foam core is composed of struts surrounded by cell walls. Before densification, as the struts are collapsed the opposite cell walls compress against each other. With loading continued, there is hardly any room left for further deformation of cellular structure. Then, the compression of the collapsed cellular structure occurred during densification of the core.

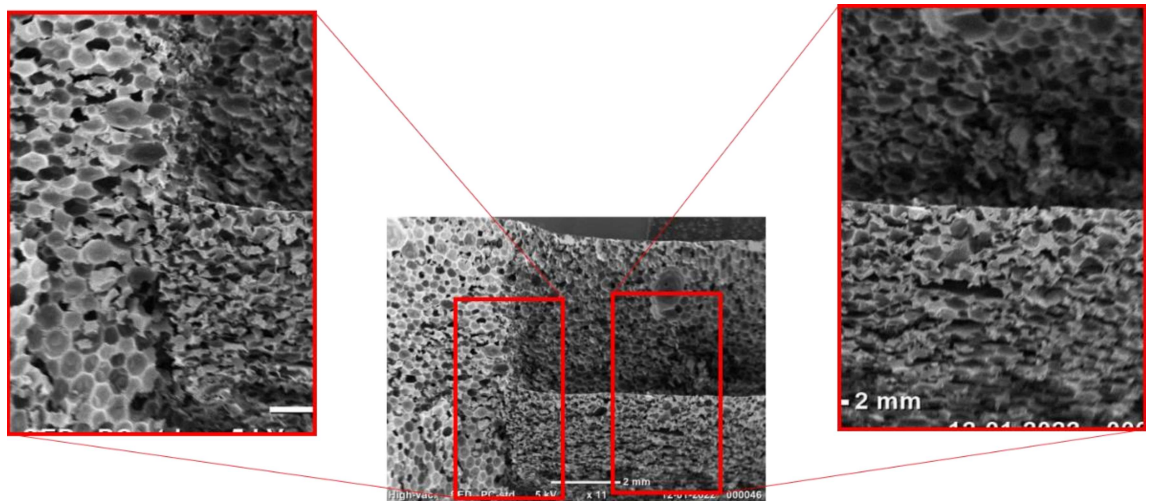


Figure 5.13 SEM image of a cross-sectional cut of 20 wt. % FA-PUF under the flat-circular indenter.

As shown in figure 5.14, the tearing initiation shift toward the center of the hemispherical indenter during loading, unlike the flat-circular indenter where the tearing line is just below the projected area of the flat circular indenter. The magnified view on the left shows the tear line defining the projected area of the PUF core for crushing while the rest of the PUF experiences compressive and shear force by the hemispherical indenter. The intact cellular structures are noticed on the bottom left side of figure 5.14. These unharmed cellular structures depict that the crushing of the core is limited to the right side of the tearing line, where the PUF core experiences densification. The magnified view on the right of figure

5.14 shows the densified FA-PUF core. Here, the crushed cell walls and collapsed struts are seen to be further compressed.

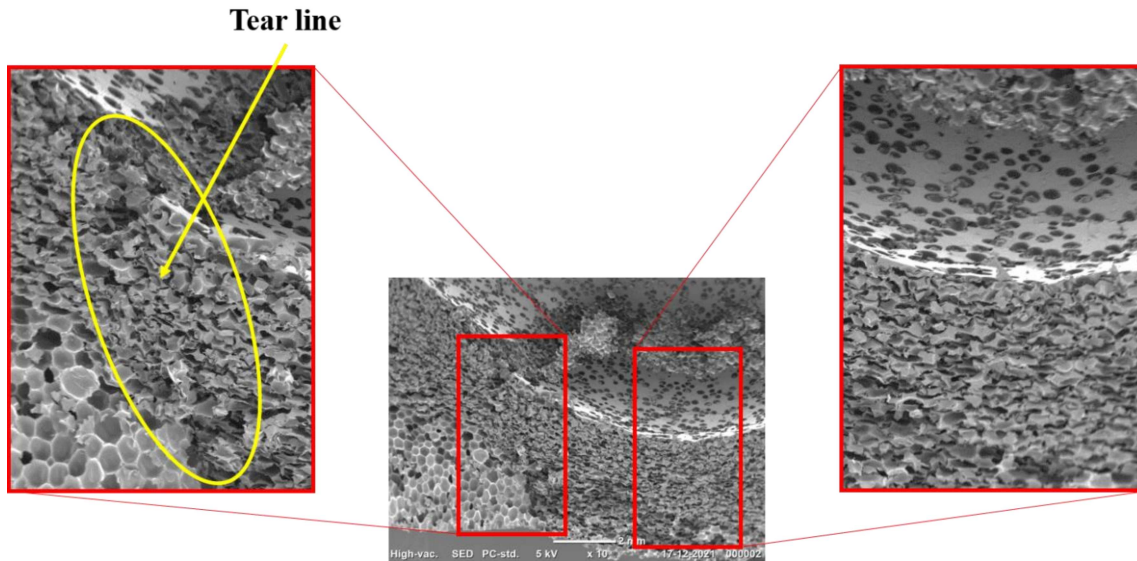


Figure 5.14 SEM image of a cross-sectional cut of 20wt. % FA-PUF under the hemispherical indenter.

The damaged PUF core's mid-cross-sectional incision is shown in figure 5.15 under the conical indenter. The sharp tip of the conical indenter tears apart the cellular FA-PUF core and punctures the cell walls. A progressive deformation through-thickness is evident in the magnified picture of figure 5.15 on the left. The PUF core was substantially deformed near the conical indenter's tip. The deformation gradually decreases when moving away from the apex of the indenter. The deformation also varies along the slant face of the conical indenter. Along the slant face of the indenter, there is a gradual core crushing, and the depth of the indentation causes more cellular structure deformation. The cell geometry collapses at higher indentation depth, whereas at the top left of the core, the cells deform elastically with intact cellular geometry. Severe tearing and core crushing are visible at the center in the magnified picture on the right of figure 5.15. The tearing line is located at the center of the deformed FA-PUF, where the cell walls are punctured and parted as the indenter travels to a higher

depth. The damage mechanisms observed can also be justified with the other FA-PUF or neat PUF configurations.

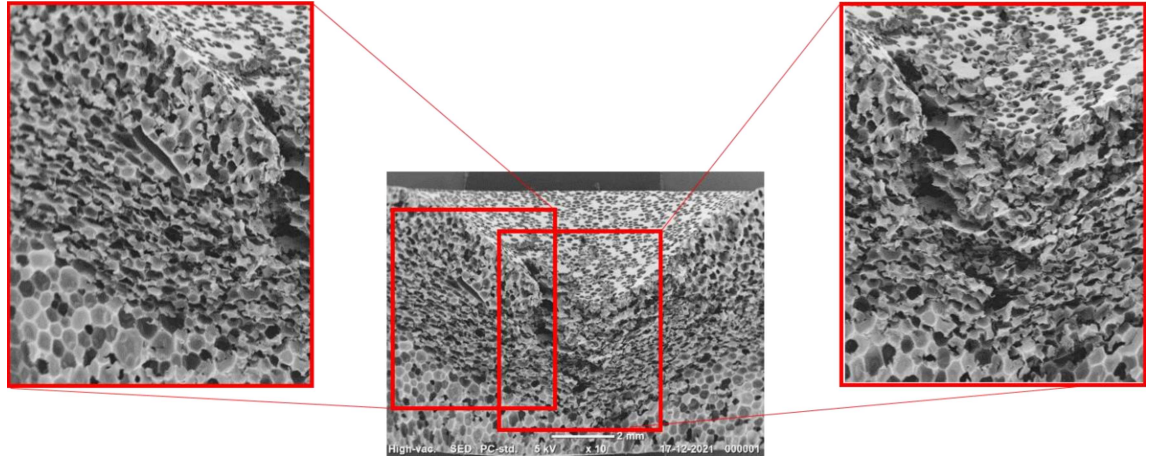


Figure 5.15 SEM image of a cross-sectional cut of 20wt. % FA-PUF under the conical indenter.

The findings conclude that the FA inclusion severely affects the indentation resistance. It was noticed that the core response changes for a particular type of nose tip indenter with FA addition. The failure and fracture of the FA-PUF core are reported to be caused by three predominant damage mechanisms: tearing, crushing, and shearing. The damage studies using optical images show that for the flat-circular and hemispherical indentation, the damage area decreases as fly ash reinforcement increases. Contrarily, the conical indentation's damage mechanism is more localised without significantly altering the affected zone. The reinforced FA-PUF core performs better, when tested with a flat-circular and hemispherical indenter. Contrary to reinforced FA-PUF, neat PUF performs pretty well under conical shape indenter. Though the damage under the projected area of the indenter gets localised, the location of the tear line shifts towards the center, when the geometry of the indenter changes from flat-circular to hemispherical and then to conical.

This Page is Intentionally Left Blank